

Testing Multi-field Inflation with Galaxy Bias

Matteo Biagetti^{*}, Vincent Desjacques[†] and Antonio Riotto[‡]

*Département de Physique Théorique and Center for Astroparticle Physics (CAP)
Université de Genève, 24 quai Ernest Ansermet, CH-1211 Genève, Switzerland*

9 August 2012

ABSTRACT

Multi-field models of inflation predict an inequality between the amplitude τ_{NL} of the collapsed limit of the four-point correlator of the primordial curvature perturbation and the amplitude f_{NL} of the squeezed limit of its three-point correlator. While a convincing detection of non-Gaussianity through the squeezed limit of the three-point correlator would rule out all single-field models, a robust confirmation or disproof of the inequality between τ_{NL} and f_{NL} would provide crucial information about the validity of multi-field models of inflation. In this paper, we discuss to which extent future measurements of the scale-dependence of galaxy bias can test multi-field inflationary scenarios. The strong degeneracy between the effect of a non-vanishing f_{NL} and τ_{NL} on halo bias can be broken by considering multiple tracer populations of the same surveyed volume. If halos down to $10^{13} M_{\odot}/h$ are resolved in a survey of volume $25(\text{Gpc}/h)^3$, then testing multi-field models of inflation at the $3\text{-}\sigma$ level would require, for instance, a detection of τ_{NL} at the level of $\tau_{\text{NL}} \sim 10^5$ given a measurement of a local bispectrum with amplitude $f_{\text{NL}} \sim 10$. However, we find that disproving multi-field models of inflation with measurements of the non-Gaussian bias only will be very challenging, unless $|f_{\text{NL}}| \gtrsim 80$ and one can achieve a halo mass resolution of $\sim 10^{10} M_{\odot}/h$.

Key words: cosmology: theory – large scale structure of the universe – inflation

1 INTRODUCTION

Inflation (see Lyth and Riotto (1999) for a review) has become the dominant paradigm for understanding the initial conditions for the large scale structure (LSS) formation and for Cosmic Microwave Background anisotropy (CMB). In the inflationary picture, primordial densities are created from quantum fluctuations “redshifted” out of the horizon during an early period of superluminal expansion of the universe, where they are “frozen”. Perturbations at the surface of last scattering are observable as temperature anisotropy in the CMB. The last and most impressive confirmation of the inflationary paradigm has been recently provided by the data of the Wilkinson Microwave Anisotropy Probe (WMAP) mission which has marked the beginning of the precision era of the CMB measurements in space (Komatsu et al. (2011)).

Despite the simplicity of the inflationary paradigm, the mechanism by which the cosmological curvature perturbation is generated is not yet fully established. In the single-

field models of inflation, the observed density perturbations are induced by fluctuations of the inflaton field itself. An alternative to the standard scenario is represented by the curvaton mechanism (Enqvist and Sloth (2002), Lyth and Wands (2002), Moroi and Takahashi (2002)) where the final curvature perturbations are produced from an initial isocurvature perturbation associated to the quantum fluctuations of a light scalar field (other than the inflaton), the curvaton, whose energy density is negligible during inflation. The curvaton isocurvature perturbations are transformed into adiabatic ones when the curvaton decays into radiation much after the end of inflation. Alternatives to the curvaton model are those models characterised by the curvature perturbation being generated by an inhomogeneity in the decay rate (Dvali and Gruzinov (2004), Kofman (2003)) of the particles responsible for the reheating after inflation. Other opportunities for generating the curvature perturbation occur at the end of inflation (Lyth (2005), Lyth and Riotto (2006)) and during preheating (Kolb et al. (2005)). A precise measurement of the spectral index n_{ζ} of the comoving curvature perturbation ζ will provide a powerful constraint to single-field models of inflation which predict the spectral index to be close to unity. However, alternative mechanisms, like the curvaton, also predict a value of

^{*} Matteo.Biagetti@unige.ch

[†] Vincent.Desjacques@unige.ch

[‡] Antonio.Riotto@unige.ch

the spectral index very close to unity. Thus, even a precise measurement of the spectral index will not allow us to efficiently distinguish among them. Furthermore, the lack of a gravity-wave signal in CMB anisotropies would not give us any information about the perturbation generation mechanism, since alternative mechanisms predict an amplitude of gravity waves far too small to be detectable by future experiments aimed at observing the B -mode of the CMB polarisation.

There is, however, a third observable which will prove fundamental in providing information about the mechanism chosen by Nature to produce the structures we see today. It is the deviation from a Gaussian statistics, *i.e.*, the presence of higher-order connected correlation functions of the perturbations. Indeed, a possible source of non-Gaussianity (NG) could be primordial in origin, being specific to a particular mechanism for the generation of the cosmological perturbations (for a review see Bartolo et al. (2004)). This is what makes a positive detection of NG so relevant: it might help discriminating among competing scenarios which, otherwise, would might remain indistinguishable.

To characterise the level of NG in the comoving curvature perturbation, one usually introduces two nonlinear parameters, f_{NL} and τ_{NL} . The first one is defined in terms of the three-point correlator, the bispectrum, of the comoving curvature perturbation in the so-called squeezed limit

$$f_{\text{NL}} = \frac{5}{12} \frac{\langle \zeta_{\vec{k}_1} \zeta_{\vec{k}_2} \zeta_{\vec{k}_3} \rangle'}{P_{\vec{k}_1}^\zeta P_{\vec{k}_2}^\zeta} \quad (k_1 \ll k_2 \sim k_3). \quad (1)$$

The second one is defined in terms of the four-point correlator, the trispectrum, in the so-called collapsed limit

$$\tau_{\text{NL}} = \frac{1}{4} \frac{\langle \zeta_{\vec{k}_1} \zeta_{\vec{k}_2} \zeta_{\vec{k}_3} \zeta_{\vec{k}_4} \rangle'}{P_{\vec{k}_1}^\zeta P_{\vec{k}_2}^\zeta P_{\vec{k}_3}^\zeta} \quad (\vec{k}_{12} \simeq 0). \quad (2)$$

We have normalised the correlators with respect to the power spectrum of the curvature perturbation,

$$\langle \zeta_{\vec{k}_1} \zeta_{\vec{k}_2} \rangle = (2\pi)^3 \delta(\vec{k}_1 + \vec{k}_2) P_{\vec{k}_1}^\zeta \quad (3)$$

and used the notation $\vec{k}_{ij} = (\vec{k}_i + \vec{k}_j)$. In all single-field models of inflation the bispectrum is suppressed in the squeezed limit and is non vanishing only when the spectral index deviates from unity, $f_{\text{NL}} = 5/12(1 - n_\zeta) \simeq 0.02$ (see Acquaviva et al. (2003), Maldacena (2003), Creminelli and Zaldarriaga (2004), Cheung et al. (2008)). A convincing detection of NG in the squeezed limit, $f_{\text{NL}} \gg 1$, would therefore rule out all single-field models (one should be aware though that, in single-field models of inflation, a large NG can be generated in shapes others than the squeezed, *e.g.* in the equilateral configuration). However, such a detection would not rule out multi-field models of inflation where the NG is seeded by light fields other than the inflaton. How can we derive some useful informations about them? In this respect, the collapsed limit of the four-point correlator is particularly important because, together with the squeezed limit of the three-point correlator, it may lead to the so-called Suyama-Yamaguchi (SY) inequality (Suyama and Yamaguchi (2008), see also Sugiyama et al. (2011), Smith et al. (2011)). Based on the conditions that 1) scalar fields are responsible for generating curvature perturbations and that 2) the fluctuations in the scalar fields at the horizon crossing are scale invariant and Gaussian,

Suyama and Yamaguchi proved the inequality

$$\tau_{\text{NL}} \geq \left(\frac{6}{5} f_{\text{NL}} \right)^2. \quad (4)$$

The condition 2) amounts to assuming that the connected three- and four-point correlations of the light fields vanish and that the NG is generated at super-horizon scales. This is quite a restrictive assumption. However, based on the operator product expansion, which is particularly powerful in characterising in their full generality the squeezed limit of the three-point correlator and the collapsed limit of the four-point correlator, it was shown that the SY inequality holds also for NG light fields (Kehagias and Riotto (2012)). This is consequence of fundamental physical principles (like positivity of the two-point function) and its hard violation would require some new non-trivial physics to be involved.

The observation of a strong violation of the inequality will then have profound implications for inflationary models. It will imply either that multi-field inflation cannot be responsible for generating the observed fluctuations independently of the details of the model, or that some new non-trivial (ghost-like) degrees of freedom play a role during inflation (Kehagias and Riotto (2012)).

Testing the SY inequality with future LSS observations and, therefore, the validity of multi-field inflationary models is the subject of this paper. The squeezed limit of the bispectrum and the collapsed limit of the trispectrum are particularly interesting from the observational point of view because they are associated to pronounced effects of NG on the clustering of dark matter halos and, in particular, to a strongly scale-dependent bias (Dalal et al. (2008)). Measurements of the galaxy power spectrum have been exploited to set limits on primordial non-Gaussianity competitive with those inferred from CMB observations (Slosar (2009), Desjacques and Seljak (2010), Xia et al. (2011)). As we have seen, a large value of f_{NL} in the squeezed limit implies that the cosmological perturbations are generated within a multi-field model of inflation where the NG is sourced by light fields other than the inflaton. An inescapable consequence of the SY inequality (4) is that the NG is also characterised by a large trispectrum in the collapsed limit. Therefore, investigations that take advantage of the scale-dependent effects of NG on the clustering of dark matter halos should in principle take into account both f_{NL} and τ_{NL} . However, since the contribution from the latter is suppressed by $10^{-4}(\tau_{\text{NL}}/f_{\text{NL}})$, setting limits on f_{NL} under the assumption $\tau_{\text{NL}} = 0$, as done in the literature, should be a good approximation unless $|\tau_{\text{NL}}| \gg f_{\text{NL}}^2$.

In this paper, we will essentially try to answer the following question: what values of f_{NL} and τ_{NL} have to be measured in order to either confirm or disprove the SY inequality? As we shall see, even though the contributions from f_{NL} and τ_{NL} are degenerate in the non-Gaussian halo bias, combining multiple halo mass bins can greatly help breaking the degeneracy. As we shall demonstrate, testing multi-field models of inflation at the $3\text{-}\sigma$ level would require, for a EUCLID-like survey, a detection of a four-point correlator amplitude in the collapsed limit of the order of $\tau_{\text{NL}} \sim 10^5$ given a measurement of a local bispectrum at the level of $f_{\text{NL}} \sim 10$. Conversely, we will argue that disproving multi-field models of inflation would require a detection of $|f_{\text{NL}}|$ at

the level of 80 or larger if dark matter halos can be resolved down to a mass $10^{10} M_\odot/h$.

The paper is organised as follows. Section 2 contains a short summary of the impact of primordial NG on the halo bias at large scales. Section 3 describes the methodology adopted. The last Section presents the results and discusses their implications. In all illustrations, the cosmology is a flat Λ CDM Universe with normalisation $\sigma_8 = 0.807$, hubble constant $h_0 = 0.701$ and matter content $\Omega_m = 0.279$.

2 NON-GAUSSIAN HALO BIAS

The effect of primordial non-Gaussianity on the halo bias can be computed through various methods such as high peaks (Matarrese and Verde (2008), Shandera et al. (2011)) or multivariate bias expansions (McDonald (2008), Giannantonio and Porciani (2008)) but, to date, the peak-background split provides the most accurate estimate of the effect (Slosar (2009), Schmidt and Kamionkowski (2010), Desjacques et al. (2011a), Smith et al. (2012), Scoccimarro et al. (2012)). As shown in Desjacques et al. (2011a), the non-Gaussian contribution to the linear bias is

$$\Delta b_1(k) = \frac{4}{(N-1)!} \frac{\mathcal{F}_s^{(N)}(k, z)}{\mathcal{M}_s(k, z)} \times \left[b_{N-2} \delta_c + b_{N-3} \left(N-3 + \frac{d \ln \mathcal{F}_s^{(N)}(k, z)}{d \ln \sigma_s} \right) \right], \quad (5)$$

where b_N are Lagrangian bias parameters, $\delta_c \sim 1.68$ is the critical threshold for (spherical) collapse and σ_s is the rms variance of the density field at redshift z smoothed on the (small) scale R_s of a halo. The linear matter density contrast $\delta_{\vec{k}}(z)$ is related to the curvature perturbation $\Phi_{\vec{k}}$ during matter domination via the Poisson equation. The latter can be expressed as $\delta_{\vec{k}}(z) = \mathcal{M}(k, z) \Phi_{\vec{k}}$, where

$$\mathcal{M}(k, z) \equiv \frac{2}{3} \frac{D(z)}{\Omega_m H_0^2} T(k) k^2. \quad (6)$$

Here, $T(k)$ is the matter transfer function, Ω_m and H_0 are the matter density in critical units and the Hubble rate today, and $D(z)$ is the linear growth rate. \mathcal{M}_s denotes $\mathcal{M}(k, z) W(kR_s)$, where $W(kR_s)$ is a spherically symmetric window function (we adopt a top-hat filter throughout this paper). Furthermore,

$$\mathcal{F}_s^{(N)}(k, z) = \frac{1}{4\sigma_s^2 P_\phi(k)} \left[\prod_{i=1}^{N-2} \int \frac{d^3 k_i}{(2\pi)^3} \mathcal{M}_s(k_i, z) \right] \mathcal{M}_s(q, z) \times \xi_\Phi^{(N)}(\vec{k}_1, \dots, \vec{k}_{N-2}, \vec{q}, \vec{k}) \quad (7)$$

is a projection factor whose k -dependence is dictated by the exact shape of the N -point function $\xi_\Phi^{(N)}$ of the gravitational potential. For the local constant- f_{NL} model, the factor $\mathcal{F}_s^{(3)}$ is equal to f_{NL} in the low k -limit (squeezed limit), so that the logarithmic derivative of $\mathcal{F}_s^{(N)}$ w.r.t. the rms variance σ_s of the small-scale density field vanishes on large scales. For all other models of primordial non-Gaussianity however, this term is significant for most relevant peak heights and becomes negligible in the high peak limit only (Desjacques et al. (2011b)). Since the halo mass function may not be universal, the non-Gaussian bias correction should in principle be computed by taking derivative of the

Table 1. Average host halo mass, number density, (Lagrangian) linear and quadratic bias factors for the low- and high-mass halo samples used in Fig.1.

	$M(M_\odot/h)$	$\bar{n} \text{ (} h^3 \text{Mpc}^{-3} \text{)}$	b_1	b_2
Halo 1	10^{12}	7×10^{-4}	0.2	-0.2
Halo 2	10^{14}	3×10^{-6}	2.5	4.5

Gaussian halo mass function w.r.t. mass (Scoccimarro et al. (2012)). However, because it is difficult to estimate such a mass derivative from real data, we will use Eq.(5), which is valid for a universal mass function. Nevertheless, one should bear in mind that non-universality can induce additional corrections at the $\sim 10\%$ level (Scoccimarro et al. (2012); Matsubara (2012)). Note also that path integral extensions of the excursion set formalism (see Maggiore and Riotto (2010)) suggest that memory terms (involving N -point correlators of the density field smoothed on any scale between R_s and R_l) could also contribute at some level (D'Aloisio et al. (2012); Ashead et al. (2012)).

Specialising the above result to the bispectrum and trispectrum shapes considered here, the non-Gaussian bias correction reads

$$\Delta b_1(k) = 2f_{\text{NL}} \frac{\delta_c b_1}{\mathcal{M}_s(k)} + \frac{1}{2} \left(g_{\text{NL}} + \frac{25}{27} \tau_{\text{NL}} \right) \times \frac{\sigma_s^2 S_{s,\text{loc}}^{(3)}}{\mathcal{M}_s(k)} \left[b_2 \delta_c + b_1 \left(1 + \frac{d \ln S_{s,\text{loc}}^{(3)}}{d \ln \sigma_s} \right) \right], \quad (8)$$

where b_1, b_2 are the first- and second-order Lagrangian bias parameters, g_{NL} is another NG coefficient parametrising the NG arising from a cubic third-order term in the curvature perturbation ζ and $S_{s,\text{loc}}^{(3)}(M)$ is the skewness of the density field in a local, quadratic non-Gaussian model with $f_{\text{NL}} = 1$. Strictly speaking, this expression is valid in the limit $k \ll 1$ only since we have ignored the k -dependence of $\mathcal{F}_s^{(4)}$. However, deviations become significant only for $k \gtrsim 0.1$ where the non-Gaussian signal is negligible and the signal-to-noise saturates (Sefusatti et al. (2011)). In linear theory, the product $\sigma_s S_{s,\text{loc}}^{(3)}(M)$ is independent of redshift. Therefore, at fixed values of b_1 and b_2 , the non-Gaussian correction induced by f_{NL} scales as $D(z)^{-1}$, whereas that induced by g_{NL} and τ_{NL} does not have any extra dependence on redshift. For the cosmology considered here, the empirical relation $\sigma_s S_{s,\text{loc}}^{(3)} \approx 3.08 \times 10^{-4} \sigma_s^{0.145}$ accurately reproduces the mass dependence of the skewness (Desjacques et al. (2011a)). The relative amplitude of the τ_{NL} -induced scale-dependent bias thus is $(\tau_{\text{NL}}/f_{\text{NL}})10^{-4}$. Whereas it is negligible in single-field inflation, it can be significant for models with $|\tau_{\text{NL}}| \gg f_{\text{NL}}^2$. Note that current limits from the CMB trispectrum are $-0.6 < \tau_{\text{NL}}/10^4 < 3.3$ (Smidt et al. (2010)).

An important feature of the NG bias correction is that its scale-dependence is degenerate in f_{NL} , τ_{NL} and g_{NL} in the large scale limit, since all the k -dependence is then located in $\mathcal{M}_s(k) \sim 1/k^2$. This degeneracy can be partly broken by considering galaxy populations tracing halos of different mass and, possibly, at different redshifts. While recent studies have analysed the problem of detecting NG through future large-scale surveys combining a number of observational datasets with simple models where only f_{NL} is nonzero and

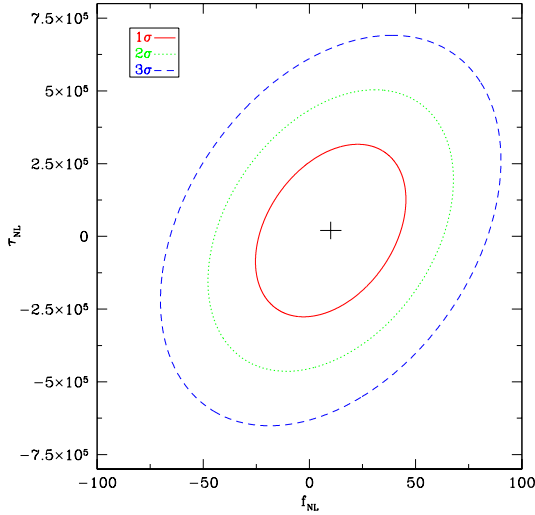


Figure 1. Confidence ellipses obtained by combining the low- and high-mass sample, assuming $f_{\text{NL}} = 10$ and $\tau_{\text{NL}} = 2 \times 10^4$.

the other two nonlinear parameters are set to zero, we will assume here that both f_{NL} and τ_{NL} are non-vanishing since we aim at testing the SY inequality (4). We will however set g_{NL} to zero¹. We refer the reader to Roth and Porciani (2012) for a recent study in which both f_{NL} and g_{NL} are nonzero. Finally, it is worth mentioning that our Eq.(8) is different from the expression given in Gong and Yokoyama (2011), who neglected the mass-dependence of the skewness.

3 METHOD

In order to assess the ability of forthcoming experiments to test the SY inequality through the measurement of the large scale bias, we use of the Fisher information content on f_{NL} and τ_{NL} from the two-point statistics of halos and dark matter in Fourier space. The Fisher matrix formalism has been extensively applied to predict how well galaxy surveys will constrain the nonlinear parameter f_{NL} (e.g., Dalal et al. (2008), Carbone et al. (2008), Cunha et al. (2010)). In particular, combining differently biased tracers of the same surveyed volume and weighting halos by mass can help mitigate the effect of cosmic variance and shot noise and, therefore, reduce the uncertainty on f_{NL} (Seljak (2009), Slosar (2009), Seljak et al. (2009), Hamaus et al. (2011)).

3.1 Fisher matrix formalism

Here and henceforth, we closely follow the notation of Hamaus et al. (2011) and define the halo overdensity in Fourier space as a vector, every element corresponding to halos with different mass bins

$$\delta_h = (\delta_h(M_1), \delta_h(M_2), \dots, \delta_h(M_n))^T. \quad (9)$$

¹ Notice that this assumption also gets rid of potentially large one-loop corrections to the SY inequality (Tasinato et al. (2012)). These corrections would be anyway below the errors we will estimate on τ_{NL} even for g_{NL} as large as 10^6 .

Assuming the halos to be locally biased and stochastic tracers of the dark matter density field δ , we can write the overdensity of halos as

$$\delta_h = \mathbf{b} \delta + \epsilon, \quad (10)$$

where \mathbf{b} is a vector whose i -component is the (Eulerian) bias of the i -th sample,

$$b_i^E(k, M_i, z) = 1 + b_1(M_i, z) + \Delta b_1(k, M_i, z), \quad (11)$$

and ϵ is a residual noise-field with zero mean. We assume that it is uncorrelated with the dark matter.

Computing the Fisher information requires knowledge of the covariance matrix of the halo samples,

$$\mathbf{C}_h = \langle \delta_h \delta_h^T \rangle = \mathbf{b} \mathbf{b}^T P + \mathbf{E}. \quad (12)$$

The brackets indicate the average within a k -shell in Fourier space. $P = \langle \delta^2 \rangle$ is the non-linear dark matter power spectrum which, on large scales, can be assumed independent of f_{NL} and τ_{NL} and $\mathbf{E} = \langle \epsilon \epsilon^T \rangle$ is the shot-noise matrix. We will follow the general treatment of Hamaus et al. (2011) and assume that \mathbf{E} is not simply diagonal with entries consistent with Poisson noise (see §3.2 for explicit expressions).

In order to simultaneously constrain f_{NL} and τ_{NL} , it is pretty clear that at least two different halo samples are required to break some of the parameter degeneracies, since the bias coefficients b_1 , b_2 , the rms variance σ_s and the skewness $S_{s,\text{loc}}^{(3)}$ have distinct mass dependences (as is apparent from the numerical fits of De Simone et al. (2011) or Enqvist et al. (2011)). More precisely, the Fisher matrix takes the following general form

$$\mathcal{F}_{ij} = V_{\text{surv}} f_{\text{sky}} \int \frac{dk k^2}{2\pi^2} \frac{1}{2} \text{Tr} \left(\frac{\partial \mathbf{C}_h}{\partial \theta_i} \mathbf{C}_h^{-1} \frac{\partial \mathbf{C}_h}{\partial \theta_j} \mathbf{C}_h^{-1} \right), \quad (13)$$

where θ_i are the parameters whose error we wish to forecast. The integral over the momenta runs from $k_{\text{min}} = \pi/(V_{\text{surv}})^{1/3}$ to $k_{\text{max}} = 0.1 \text{ Mpc}^{-1}/h$, where V_{surv} is the surveyed volume and f_{sky} is the fraction of the sky observed. For illustration purposes, we will adopt the specifications of an EUCLID-like experiment: $V_{\text{surv}} f_{\text{sky}} = 25 \text{ Gpc}^3/h^3$ at median redshift $z = 0.7$. We will ignore the redshift evolution and assume that all the surveyed volume is at that median redshift. In principle however, it should be possible to extract additional information on the non-Gaussian bias from the redshift dependence of the survey. For a single mass bin, the four entries of the Fisher matrix have the same k -dependence at low- k . As a consequence, the determinant is very close to zero and, therefore, yields large (marginalised) errors. In this case, it is impossible to test the SY inequality regardless the characteristics of the halo sample, unless one has some prior on one of the parameters.

In the general case of N halo populations, the entries of the halo covariance matrix read $(a, b = 1, \dots, N)$

$$C_{ab} = b_1^E(k, M_a, z) b_1^E(k, M_b, z) P(k) + E_{ab}. \quad (14)$$

The derivative of the halo covariance matrix with respect to some parameter θ is

$$\frac{\partial C_h}{\partial \theta} = (\mathbf{b}_\theta \mathbf{b}^T + \mathbf{b} \mathbf{b}_\theta^T) P, \quad (15)$$

where $\mathbf{b}_\theta = \partial \mathbf{b} / \partial \theta$. We have ignored the dependence of \mathbf{E} on θ as it is expected to be small for f_{NL} and τ_{NL} . Following Hamaus et al. (2011), the inverse of the covariance matrix

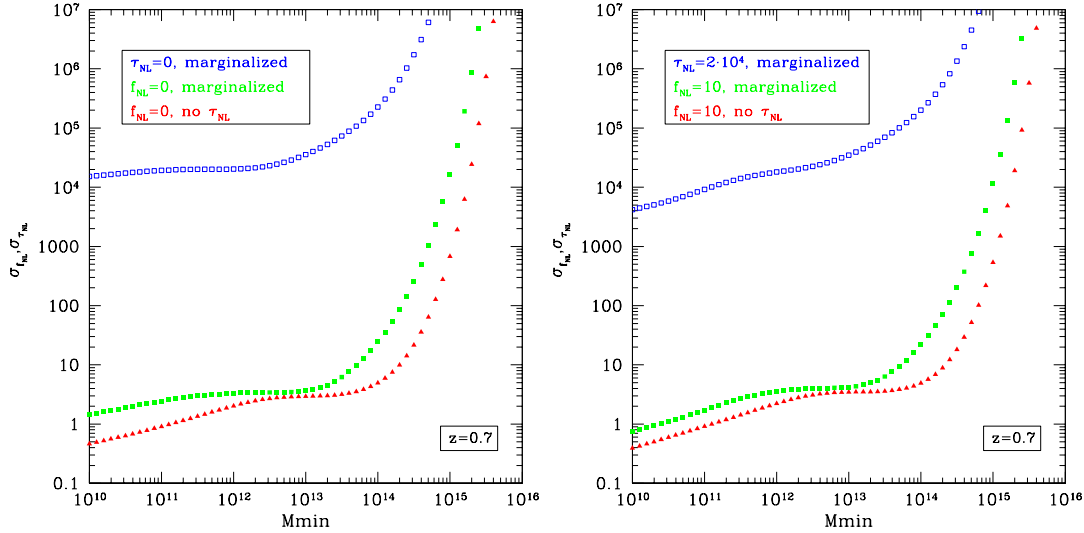


Figure 2. Halo model predictions for the $1\text{-}\sigma$ errors as a function of minimum halo mass in the limit of $N \gg 1$ halo mass bins with identical number density. Red triangles show the uncertainty on f_{NL} for a one-parameter model with $f_{\text{NL}} = 0$ (left panel) and $f_{\text{NL}} = 10$ (right panel). Filled (green) and empty (blue) squares represent the $1\text{-}\sigma$ uncertainties on f_{NL} and τ_{NL} for the two-parameters fiducial models $(f_{\text{NL}}, \tau_{\text{NL}}) = (0, 0)$ (left panel) and $(f_{\text{NL}}, \tau_{\text{NL}}) = (10, 2 \times 10^4)$ (right panel).

Table 2. $1\text{-}\sigma$ errors obtained with $N \gg 1$ halo mass bins with $M > M_{\text{min}}$. Top and bottom rows show results for $M_{\text{min}} = 10^{13}$ and $10^{10} M_{\odot}/h$, respectively.

	$f_{\text{NL}} = 0$ no τ_{NL}	$f_{\text{NL}} = 10$ no τ_{NL}	$f_{\text{NL}} = 0$ $\tau_{\text{NL}} = 0$	$f_{\text{NL}} = 10$ $\tau_{\text{NL}} = 2 \times 10^4$
$\sigma_{f_{\text{NL}}}$	2.9	3.4	3.6	4.2
$\sigma_{\tau_{\text{NL}}}$	—	—	3.6×10^4	3.4×10^4
$\sigma_{f_{\text{NL}}}$	0.5	0.4	1.4	0.8
$\sigma_{\tau_{\text{NL}}}$	—	—	1.5×10^4	0.4×10^4

can be obtained using the Sherman-Morrison formula (see Sherman and Morrison (1950) and Bartlett (1951))

$$\mathbf{C}_h^{-1} = \mathbf{E}^{-1} - \frac{\mathbf{E}^{-1} \mathbf{b} \mathbf{b}^{\top} \mathbf{E}^{-1} P}{1 + \mathbf{b}^{\top} \mathbf{E}^{-1} \mathbf{b} P}. \quad (16)$$

On inserting the expression (15) into Eq. (13), we can write down the Fisher matrix for two generic parameters θ_i ($i = 1, 2$) as

$$\mathcal{F}_{ij} = \frac{P^2}{2} \text{Tr} \left[(\mathbf{b} \mathbf{b}_i^{\top} + \mathbf{b}_i \mathbf{b}^{\top}) \mathbf{C}_h^{-1} (\mathbf{b} \mathbf{b}_j^{\top} + \mathbf{b}_j \mathbf{b}^{\top}) \mathbf{C}_h^{-1} \right]. \quad (17)$$

The elements of the Fisher matrix can be easily expressed in terms of the following quantities

$$\begin{aligned} \alpha &= \mathbf{b}^{\top} \mathbf{E}^{-1} \mathbf{b} P \\ \beta_i &= \mathbf{b}^{\top} \mathbf{E}^{-1} \mathbf{b}_{\theta_i} P \\ \gamma_{ij} &= \mathbf{b}_{\theta_i}^{\top} \mathbf{E}^{-1} \mathbf{b}_{\theta_j} P. \end{aligned} \quad (18)$$

After some algebra, we obtain

$$\mathcal{F}_{ij} = \frac{\alpha \gamma_{ij} + \beta_i \beta_j + \alpha (\alpha \gamma_{ij} - \beta_i \beta_j)}{(1 + \alpha)^2}, \quad (19)$$

which generalises the calculation reported in Hamaus et al. (2011). Note that, in what follows, $\theta_1 = f_{\text{NL}}$ and $\theta_2 = \tau_{\text{NL}}$.

One should bear in mind the caveat that the present Fisher matrix analysis assumes Gaussian uncertainties, even

though it is likely that the estimators \hat{f}_{NL} and $\hat{\tau}_{\text{NL}}$ have non-Gaussian distributions. One possible way of testing this assumption would be to generate Monte-Carlo simulations of the halo samples, but this is beyond the scope of this paper.

3.2 Halo model predictions

Even though the halo model makes a number of predictions that are not physically sensible (such as a white noise contribution in the limit $k \rightarrow 0$ of the cross halo-mass power spectrum), it was shown to furnish a very good fit to the eigenvalues and eigenvectors of the halo stochasticity matrix (Hamaus et al. (2010)). In this model, the shot-noise matrix can be cast into the closed form expression \mathbf{E} ,

$$\mathbf{E} = \bar{n} \mathbf{I} - \mathbf{b} \mathcal{M}^{\top} - \mathcal{M} \mathbf{b}^{\top}. \quad (20)$$

Here, $\mathcal{M} = \mathbf{M}/\bar{\rho}_m - \mathbf{b} \langle n \mathbf{M}^2 \rangle / 2 \bar{\rho}_m^2$, \mathbf{M} is a vector whose entries are the halo masses and $n = n(M)$ is the number density of halos of mass M . The Poisson expectation is recovered upon setting $\mathcal{M} = 0$. In the limit of $N \gg 1$ halo mass bins with identical number density \bar{n} , we can replace the scalar products by integrals. A straightforward calculation shows that the coefficients α , β_i and γ_{ij} can be rewritten as

$$\alpha = \frac{\langle b^2 \rangle}{(\bar{n}_{\text{tot}}^{-1} - \langle \mathcal{M} b \rangle)^2 - \langle b^2 \rangle \langle \mathcal{M}^2 \rangle} \bar{n}_{\text{tot}}^{-1} P \quad (21)$$

$$\beta_i = \frac{\langle b b_{\theta_i} \rangle (\bar{n}_{\text{tot}}^{-1} - \langle \mathcal{M} b \rangle) + \langle b^2 \rangle \langle \mathcal{M} b_{\theta_i} \rangle}{(\bar{n}_{\text{tot}}^{-1} - \langle \mathcal{M} b \rangle)^2 - \langle b^2 \rangle \langle \mathcal{M}^2 \rangle} P \quad (22)$$

$$\begin{aligned} \gamma_{ij} &= \langle b_{\theta_i} b_{\theta_j} \rangle \bar{n}_{\text{tot}} P \\ &+ \frac{\langle b^2 \rangle \langle \mathcal{M} b_{\theta_i} \rangle \langle \mathcal{M} b_{\theta_j} \rangle + \langle \mathcal{M}^2 \rangle \langle b b_{\theta_i} \rangle \langle b b_{\theta_j} \rangle}{(\bar{n}_{\text{tot}}^{-1} - \langle \mathcal{M} b \rangle)^2 - \langle b^2 \rangle \langle \mathcal{M}^2 \rangle} \bar{n}_{\text{tot}} P \\ &+ \frac{(\langle b b_{\theta_i} \rangle \langle \mathcal{M} b_{\theta_j} \rangle + \langle b b_{\theta_j} \rangle \langle \mathcal{M} b_{\theta_i} \rangle) (\bar{n}_{\text{tot}}^{-1} - \langle \mathcal{M} b \rangle)}{(\bar{n}_{\text{tot}}^{-1} - \langle \mathcal{M} b \rangle)^2 - \langle b^2 \rangle \langle \mathcal{M}^2 \rangle} \bar{n}_{\text{tot}} P \end{aligned} \quad (23)$$

where

$$\langle xy \rangle \equiv \frac{1}{\bar{n}_{\text{tot}}} \int_{M_{\min}}^{M_{\max}} dM n(M) x(M) y(M) \quad (24)$$

$$\bar{n}_{\text{tot}} \equiv \int_{M_{\min}}^{M_{\max}} dM n(M) = N \bar{n} . \quad (25)$$

Here, $n(M)$ is the halo mass function, which we assume to be of the Sheth and Tormen (1999) form with $p = 0.3$, $q = 0.73$ and a normalisation $A = 0.322$. This yields $\langle n M^2 \rangle / \bar{\rho}_m^2 = 75.9 \text{Mpc}^3 / h^3$ at redshift $z = 0.7$.

4 RESULTS AND CONCLUSIONS

We first compute the uncertainties on f_{NL} and τ_{NL} from two different tracer populations and for a shot-noise matrix consistent with Poisson noise, i.e. $\mathbf{E} = \text{diag}(1/n(M_1), 1/n(M_2))$. We consider a nearly unbiased sample with average mass $M \sim 10^{12} M_{\odot}/h$ and a high mass sample with $M = 10^{14} M_{\odot}/h$. Table 1 summaries the characteristics of these populations. For a given mass M , the second-order Lagrangian bias parameter $b_2(M)$ is computed from the Sheth-Tormen multiplicity function, whereas the skewness $S_{s,\text{loc}}^{(3)}$ is computed from the phenomenological relation given in §2. Fig. 1 shows the resulting 68, 95 and 99% confidence contours for the parameters f_{NL} and τ_{NL} when the fiducial model assumes $f_{\text{NL}} = \pm 10$ and $\tau_{\text{NL}} = 2 \times 10^4$. The 1- σ errors are $\sigma_{f_{\text{NL}}} \simeq 23$ and $\sigma_{\tau_{\text{NL}}} \simeq 2.0 \times 10^5$. We have tried different combinations of halo populations and found that the errors do not change significantly. At this point, we would conclude that galaxy bias alone cannot yield interesting constraints on τ_{NL} and f_{NL} .

The situation changes dramatically when the surveyed halos are divided into $N \gg 1$ populations of increasing mass, with equal number density. In Fig. 2, symbols represent the halo model prediction for the 1- σ uncertainties $\sigma_{f_{\text{NL}}}$ and $\sigma_{\tau_{\text{NL}}}$ in the limit of infinitely many halo bins. The shot-noise matrix now takes the form Eq.(20). Red triangles indicate $\sigma_{f_{\text{NL}}}$ in a one-parameter model with $f_{\text{NL}} = 0$ (left panel) and $f_{\text{NL}} = 10$ (right panel). Filled and empty squares represent $\sigma_{f_{\text{NL}}}$ and $\sigma_{\tau_{\text{NL}}}$ in a two-parameters model with $(f_{\text{NL}}, \tau_{\text{NL}}) = (0, 0)$ (left panel) and $(f_{\text{NL}}, \tau_{\text{NL}}) = (10, 2 \times 10^4)$ (right panel). Results are shown as a function of the mass of the smallest halos resolved in the survey. Compared to the previous configuration, significant gains are already achieved for $M_{\min} \approx 10^{13} M_{\odot}/h$. While the constraint on f_{NL} is somewhat degraded if one allows for a non-zero τ_{NL} , the 1- σ uncertainty on τ_{NL} is of the order of $(10^3 - 10^4)$, an order of magnitude better than in the case of two galaxy populations. Table 2 gives the 1- σ errors for $M_{\min} = 10^{13}$ and $10^{10} M_{\odot}/h$.

How well can we test the SY inequality with galaxy bias? Fig. 3 displays, as a function of f_{NL} , the minimum value of τ_{NL} for which the difference $(\tau_{\text{NL}} - (36/25)f_{\text{NL}}^2)$ is greater than its 1-, 2- and 3- σ error which, for Gaussian-distributed f_{NL} and τ_{NL} , reads

$$\begin{aligned} \sigma_{\tau_{\text{NL}} - \frac{36}{25}f_{\text{NL}}^2}^2 &= \sigma_{\tau_{\text{NL}}}^2 + 2 \left(\frac{36}{25} \right)^2 \sigma_{f_{\text{NL}}, \tau_{\text{NL}}}^2 \\ &+ 4 \left(\frac{36}{25} \right)^2 \sigma_{f_{\text{NL}}}^2 \bar{f}_{\text{NL}}^2 - 4 \left(\frac{36}{25} \right) \sigma_{f_{\text{NL}}, \tau_{\text{NL}}} \bar{f}_{\text{NL}} , \end{aligned} \quad (26)$$

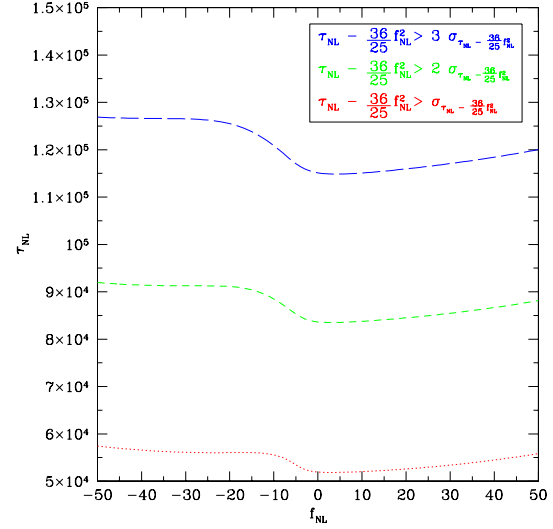


Figure 3. Testing the validity of the SY inequality with measurements of the non-Gaussian bias. The various curves are halo model predictions for $N \gg 1$ halo mass bins with $M_{\min} = 10^{13} M_{\odot}/h$. At fixed value of f_{NL} , they indicate the minimum τ_{NL} required in order to have a measurement of the SY inequality at the 1-, 2- and 3- σ confidence level.

where $\sigma_{f_{\text{NL}}}^2$, $\sigma_{f_{\text{NL}}, \tau_{\text{NL}}}$ and $\sigma_{\tau_{\text{NL}}}^2$ are the entries of the inverted Fisher matrix and \bar{f}_{NL} , $\bar{\tau}_{\text{NL}}$ are the values of the fiducial model assumed. The various curves indicate the halo model prediction for $N \gg 1$ halo populations with a minimum resolved mass $M_{\min} = 10^{13} M_{\odot}/h$. For instance, if a non-vanishing value of $f_{\text{NL}} = 10$ is measured in the future, then the contribution induced by the collapsed limit of the trispectrum must be detected with an amplitude of at least $\tau_{\text{NL}} \sim \mathcal{O}(1) \times 10^5$ in order to have a 3- σ detection of the SY inequality with the non-Gaussian halo bias. Of course, these values are only indicative since the analysis is performed with the restrictive assumption of Gaussian errors.

Finally, we can also assess how well galaxy bias can probe the violation of the SY inequality. As stated above, the observation of a strong violation would have profound implications for inflationary models as it implies either that multi-field inflation, independently of the details of the model, cannot be responsible for generating the observed fluctuations, or that some new non-trivial (ghost-like) degrees of freedom play a role during inflation. Measuring a violation essentially consists in a simultaneous detection of a non-zero value of f_{NL} and a (non-zero) small enough value of τ_{NL} . Here, we have simply estimated the smallest $|f_{\text{NL}}|$ such that $(36/25)f_{\text{NL}}^2$ is larger than the 3- σ error on τ_{NL} . Having found that, for the current observationally allowed range of f_{NL} , the error of τ_{NL} does not significantly change if we set in all runs $\tau_{\text{NL}} = 0$, we have thus computed $\sigma_{\tau_{\text{NL}}}$ assuming a vanishing value of τ_{NL} . A comparison of $3\sigma_{\tau_{\text{NL}}}$ with $(36/25)f_{\text{NL}}^2$ shows that, for a minimum halo mass $M_{\min} = 10^{13} M_{\odot}/h$, the SY inequality cannot be tested with the non-Gaussian galaxy bias solely for realistic values of f_{NL} . Even if halos are resolved down to $10^{10} M_{\odot}/h$ is $3\sigma_{\tau_{\text{NL}}} < (36/25)f_{\text{NL}}^2$ satisfied only for $|f_{\text{NL}}|$ larger than ~ 80 .

Summarising, a large NG in the squeezed limit implies that the cosmological perturbations are generated by some light scalar field other than the inflaton. The SY in-

equality (4) inevitably imposes that a large trispectrum in the collapsed limit is also present. However, the contribution of τ_{NL} to the non-Gaussian halo bias is suppressed by $10^{-4}(\tau_{\text{NL}}/f_{\text{NL}})$ and strongly degenerate with that induced by f_{NL} . Notwithstanding this, we have shown that multi-tracer methods can exploit the distinct mass-dependence of the f_{NL} - and τ_{NL} -induced bias corrections to reduce the $1\text{-}\sigma$ uncertainty down to $\sigma_{\tau_{\text{NL}}} \lesssim 10^4$ (and simultaneously achieve $\sigma_{f_{\text{NL}}} \sim 1 - 5$) for a survey covering half of the sky up to $z \approx 1$. The exact values depend on the mass M_{min} of the least massive halos observed. Our results on the capability of testing the SY inequality through the NG scale-dependent bias are summarised in Fig.3. The latter shows that testing the SY inequality at the level of $3\text{-}\sigma$ would require detecting τ_{NL} at the level of 10^5 for the minimum resolved mass $M_{\text{min}} = 10^{13} M_{\odot}/h$. Conversely, testing the violation of the SY inequality requires both a much smaller resolved mass, $M_{\text{min}} = 10^{10} M_{\odot}/h$ and a large bispectrum, $|f_{\text{NL}}| \gtrsim 80$. As mentioned above, all these results are valid provided that $g_{\text{NL}} = 0$ and that the nonlinear parameters f_{NL} and τ_{NL} estimated from the data are Gaussian-distributed. Relaxing these assumptions will be the subject of future work.

ACKNOWLEDGEMENTS

We thank Licia Verde for comments on an early version of this manuscript, and Uroš Seljak for discussions. M.B. and V.D. acknowledge support by the Swiss National Science Foundation. A.R. is supported by the Swiss National Science Foundation, project ‘The non-Gaussian Universe’ (project number: 200021140236).

REFERENCES

- Acquaviva V., Bartolo N., Matarrese S. & Riotto A., 2003, Nucl. Phys. B **667**, 119.
- Ashead P., Baxter E.J., Dodelson S. & Lidz A., 2012, arXiv:1206.3306.
- Assassi V., Baumann D. & Green D., 2012, arXiv:1204.4207 [hep-th].
- Bartlett M.S., 1951, Ann. Math. Stat. **22**, 107.
- Bartolo N., Komatsu E., Matarrese S. & Riotto A., 2004, Phys. Rept. **402**, 103.
- Bartolo N. & Riotto A., 2009, JCAP **0903**, 017.
- Tasinato G., Byrnes C., Nurmi S. & Wands D., 2012, arXiv:1207.1772 [hep-th].
- Carbone C., Verde L. & Matarrese S., 2008, Astrophys. J. **684**, L1.
- Cheung C., Fitzpatrick L., Kaplan J. & Senatore L., 2008, JCAP **0802**, 021.
- Chongchitnan S. & Silk J., 2010, Astrophys. J. **724**, 285.
- Cremineilli P. & Zaldarriaga M., 2004, JCAP **0410**, 006.
- Cunha C., Huterer D. & Doré O., 2010, Phys. Rev. D **82**, 023004.
- Dalal N., Dore O., Huterer D. & Shirokov A., 2008, Phys. Rev. D **77**, 123514.
- D’Aloisio A., Zhang J., Jeong D. & Shapiro P.R., 2012, arXiv:1206.3305.
- De Simone A., Maggiore M. & Riotto A., 2011, Mon. Not. Roy. Astron. Soc. **412**, 2587.
- Desjacques V. & Seljak U., 2010, Phys. Rev. D **81**, 023006.
- Desjacques V., Jeong D. & Schmidt F., 2011a, Phys. Rev. D **84**, 063512.
- Desjacques V., Jeong D. & Schmidt F., 2011b, Phys. Rev. D **84**, 061301.
- Dvali G. & Gruzinov A., 2004, Phys. Rev. D **69**, 023505.
- Enqvist K. & Sloth M., 2002, Nucl. Phys. B **626**, 395.
- Enqvist K., Hotchkiss S. & Taanila O., 2011, JCAP **1104**, 017.
- Giannantonio T. and Porciani C., 2010, Phys. Rev. D **81**, 063530.
- Gong J.-O. and Yokoyama S., 2011, Mon. Not. Roy. Astron. Soc. **417**, L79.
- Hamaus N., Seljak U., Desjacques V., Smith R.E., Baldauf T., 2010, Phys. Rev. D **82**, 043515.
- Hamaus N., Seljak U. & Desjacques V., 2009, Phys. Rev. D **84**, 083509.
- Kehagias A. & Riotto A., 2012, arXiv:1205.1523 [hep-th], to be published in Nucl. Phys. B.
- Kofman L., 2004, arXiv:astro-ph/0303614.
- Kolb E.W., Riotto A. & Vallinotto A., 2005, Nucl. Phys. B **626**.
- Komatsu R. & Spergel D.N., 2001, Phys. Rev. D **63**, 063002.
- Komatsu E. *et al.* [WMAP Collaboration], 2011 Astrophys. J. Suppl. **192**, 18.
- Lyth D. & Riotto A., 1999, Phys. Rept. **314**, 1.
- Lyth D. & Wands D., 2002, Phys. Lett. B **524**, 5.
- Lyth D., 2005, JCAP **0511**, 006.
- Lyth D. & Riotto A., 2006, Phys. Rev. Lett. **97**, 12130.
- Maggiore M. & Riotto A., 2010, Astrophys. J. **711**, 907.
- Maldacena J., 2003, JHEP **0305**, 013.
- Matarrese S. & Verde L., 2008, Astrophys. J. **677**, L77.
- Matsubara T., 2012, arXiv:1206.0562.
- McDonald P., 2008, Phys. Rev. D **78**, 123519.
- Moroi T. & Takahashi T., 2002, Phys. Lett. B **522**, 215 [Erratum-ibid. B **539**, 303 (2002)].
- Roth N. & Porciani C. C., 2012, arXiv:1205.3165.
- Schmidt F. & Kamionkowski M., 2010, Phys. Rev. D **82**, 103002.
- Scoccimarro R., Hui L., Manera M. & Chan K. C., 2012, Phys. Rev. D **85**, 083002.
- Sefusatti E., Crocce M. & Desjacques V., 2011, arXiv:1111.6966.
- Seljak U., 2009, Phys. Rev. Lett. **102**, 021302.
- Seljak U., Hamaus N. & Desjacques V., 2009, Phys. Rev. Lett. **103**, 091303.
- Shandera S., Dalal N. & Huterer D., 2011, JCAP **1103**, 017.
- Sherman J. & Morrison W.J., 1950, Ann. Math. Stat. **21**, 124.
- Sheth R.K. & Tormen G., 1999, Mon. Not. Roy. Astron. Soc. **308**, 119.
- Slosar A., Hirata C.M., Seljak U., Ho S. & Padmanabhan N., 2008, JCAP **0808**, 031.
- Slosar A., 2009, JCAP **0903**, 004.
- Smidt J., Amblard A., Byrnes C. T., Cooray A., Heavens A. & Munshi D., 2010, Phys. Rev. D **81**, 123007.
- Smith K.M., Lo Verde M. & Zaldarriaga M., 2011, Phys. Rev. Lett. **107**, 191301.
- Smith K. M., Ferraro S. & LoVerde M., 2012, JCAP **0312**, 032.

- Sugiyama N.S., Komatsu E. & Futamase T., 2011, Phys. Rev. Lett. **106**, 251301.
Suyama T. & Yamaguchi M., 2008, Phys. Rev. D **77**, 023505.
Xia J.-Q., Baccigalupi C., Matarrese S., Verde L. and Viel M., 2011, JCAP**0811**, 033.